The Role of BPA in Cellular Stress and Incidence of Reproductive Cancers

A Major Qualifying Project Submitted to the Faculty of Worcester Polytechnic institute
In partial fulfillment of the requirements for the Degree of Bachelor of Science
By:

_____
Hope Hutchinson

Date: April 27, 2023
Approved:

_____
Professor Natalie Farny, Advisor

_____
Professor Brenton Faber, Advisor

Table of Contents

Table of Figures

Project Description

This Major Qualifying Project (MQP) was completed to satisfy the requirements of both the Biology & Biotechnology and Professional Writing degrees. The purpose of this project was to expand on current knowledge in the field of stress granule biology as well as apply this knowledge to public health through conduction of an epidemiological study. These studies worked collaboratively to contribute to the field of stress granule biology and lay the groundwork for further studies into the implications of bisphenol analogue exposure and stress granule formation on human health. To complete this combined MQP, I conducted lab work studying stress granule formation in response to BPA under the guidance of Dr. Natalie Farny and conducted an epidemiological study on the incidence of female reproductive cancers in correlation with socioeconomic status in NY state under the guidance of Dr. Brenton Faber.

This full MQP report is a compilation of the work completed for both majors, written by myself.

Acknowledgements

Biology & Biotechnology MQP

I would like to thank Yizhe Ma, WPI graduate student in the Biology and Biotechnology department, for the wt-U2OS cells as well as assistance throughout the project. I would also like to thank Alexandra Cabral, WPI graduate student in the Biology and Biotechnology department, for her assistance throughout the project. I would like to extend a special thank you to Dr. Natalie Farny for her guidance and support throughout the MQP process.

Professional Writing MQP

I would like to thank the state of New York for allowing public access to state health records through their online portal. I would like to thank Ronit Avadhuta for his help in running statistical analysis on the obtained data. Finally, I would especially like to thank Dr. Brenton Faber for his guidance and support throughout the development of this MQP.

Chapter 1: Stressed Out! Role of GPER1 in BPA-Induced Stress Granule Formation and Incidence of Female Reproductive Cancers in Correlation with Socioeconomic Status in NY State as a Marker of BPA Exposure

Abstract

Bisphenol A (BPA) is a component of polycarbonate plastics and epoxy resins that activates the cellular stress response, triggering formation of stress granules (SGs). The pathway of BPA-induced SG formation has yet to be elucidated. It was hypothesized that BPA induces SGs through GPER1, a G protein coupled estrogen receptor. Use of an agonist (G1) and antagonist (CIMBA) suggest that GPER1 plays a role in BPA-induced SGs. SGs are believed to be cytoprotective. Repeat exposure to BPA is thought to compromise this protective mechanism, leading to increased disease risk. An epidemiologic study was conducted to examine the relationship between female reproductive cancers (FRCs) and socioeconomic status as a marker of BPA exposure, and a linear relationship was observed in NY state.

Introduction

Overview of BPA and bisphenol analogues

Bisphenol A, also known as BPA, is a synthetic chemical widely used in the production of polycarbonate plastics, epoxy resins, and other consumer products such as toys, electronics, and medical supplies (Chen, Kannan, Tan, et al, 2019). While bisphenol analogues differ in their overall chemical structure, all contain two hydroxyphenyl groups, as shown in Figure 1, and are utilized in commercial manufacturing for similar purposes. The image to the right shows the chemical structures of BPA and several common bisphenol analogues (Chen, Kannan, Tan, et al, 2019). Bisphenol analogues have grown in use as an alternative to BPA due to the implementation of policies banning BPA in consumer products for its observed effects on human health.

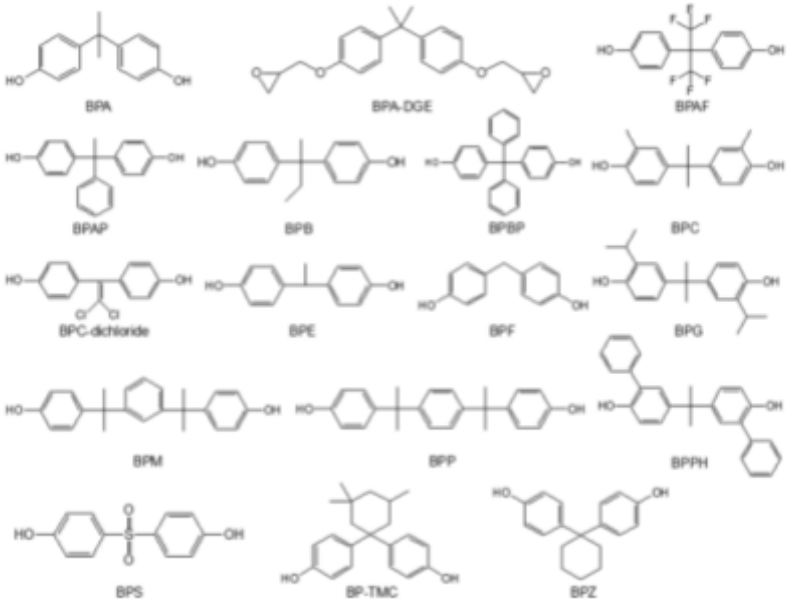

Figure 1. Chemical structures of BPA and bisphenol analogues. Reproduced from Chen et. al., 2019.

BPA has been described as an estrogen-mimicking endocrine disruptor (EED), although the exact mechanism of endocrine disruption is unknown. Exposure to EEDs is associated with many adverse health conditions, such as male and female infertility, polycystic ovarian syndrome (PCOS), and estrogen-dependent cancers. Human exposure to bisphenols occurs predominantly through dermal contact and hand-to-mouth transfer of products containing bisphenols. Research suggests that dietary sources of bisphenols may increase exposure by at least one order of magnitude when compared to non-dietary sources (e.g. dermal contact and spatial proximity). This contamination of food with bisphenols often occurs through contact between foodstuffs and their containers, such as with canned foods. Biomonitoring of human bisphenol exposure is primarily conducted via urinalysis and blood serum assessment (Chen, Kannan, Tan, et al, 2019).

Prior Research

In 2016, a group of researchers analyzed the results of an NHANES cross-sectional study spanning from the years 2003-2008 to examine the correlation between canned food and beverage consumption and BPA levels in the urine (Hartle, Navas-Acien, & Lawrence, 2016). This study involved routine urinalysis in conjunction with a 24-hour dietary recall of 6,372 participants over this 5 year period. Other demographics obtained include sex, age, race, Poverty Income Ratio (PIR), education, and smoking status/exposure. This study found that self-reported

consumption of canned food within 24 hours of urinalysis resulted in a statistically significant increase in urinary BPA levels for both adults and children in a dose-dependent manner. Self-reported consumption of one canned food was associated with a 24% increase in urinary BPA levels within 24 hours while self-reported consumption of two or more canned foods was associated with a 54% increase in urinary BPA levels compared to those who reported no canned food consumption. The researchers also noted differences in the exposure rate based on the type of food within the can. Compared to those who self-reported no canned food consumption, those who reported consumption of canned fruits or vegetables experienced, on average, a 41% increase in urinary BPA within 24 hours. Canned pastas were found to increase urinary BPA levels by 70% and canned soups were associated with a 229% increase. No correlation between canned beverage consumption and urinary BPA levels was identified (Hartle, Navas-Acien, & Lawrence, 2016).

Other epidemiologic studies have been conducted to assess cancer rates and exposure to carcinogens, such as through smoking, proximity to nuclear radiation, and occupational risk factors. For example, a review article relating smoking to lung cancer was published in 2012 (Lee, Forey, & Coombs, 2012). This study involved systematic review of 287 studies conducted in the 1900s containing data collected from patients diagnosed with lung cancer. Meta-data were stratified based on the following indices: type of lung cancer (e.g. squamous cell carcinoma and adenocarcinoma); smoking status (never a smoker, ex-smoker, and current smoker); type of smoking product used (e.g. cigarettes, pipes, and cigars); dose-related metrics (frequency of use, duration of use, and age of onset); and patient age, sex, and race. The researchers performed statistical analysis on various combinations of these indices to control for confounding variables and determine a correlation between smoking and lung cancer (Lee, Forey, & Coombs, 2012).

Numerous *in vivo* studies, conducted both in human cell lines and mammalian models, have found that exposure of cells to BPA results in altered cell functions that promote carcinogenesis through increased proliferation, invasion, and decreased apoptosis across several tissue types including breast, ovarian, colon, and liver (Chevalier et al., 2012; Prins et al., 2014; Ge et al., 2014; Wang et al., 2015, 2017, 2019; Ma et al., 2015; Song et al., 2015; Pfeifer et al., 2015; Jeong et al., 2017; Sauer et al,. 2017; Hui et al., 2018; Qu et al., 2018; Hanafi et al., 2019). BPA has been found to interfere with cell signaling pathways through interaction with nuclear and membrane-bound receptors, many of which are involved in reproductive and endocrine function (Khan, Correia, Adiga, et al., 2021). In this way, reproductive cancers such as breast, ovarian, and endometrial are of particular interest for those researching BPA as a carcinogen.

One observed cellular effect of BPA is its role in the formation of stress granules (SGs), which are aggregates of cytoplasmic proteins and mRNA (Fay, Columbo, Cotter, al., 2021). SGs are highly conserved among eukaryotes and form in response to inhibition of mRNA translation, which can be triggered by extracellular stressors such as heat shock, UV radiation, and oxidative

stress. SGs trigger the integrated stress response (ISR), which slows translation to conserve energy and activate downstream pathways geared toward cellular survival (Fay, Columbo, Cotter, al., 2021). BPA causes SG formation through activation of PKR-like endoplasmic reticulum kinase (PERK), although the mechanism through which BPA activates the PERK pathway is currently unknown. Chronic exposure to BPA and the associated adverse health effects may be related to the assembly of SGs and altered induction of the integrated stress response (ISR).

Integrated Stress Response and Stress Granules

The protein folding environment of the endoplasmic reticulum can be disturbed by cellular stressors, activating the unfolding protein response (UPR), which is just one component of the ISR (Cui, Li, Ron, et al., 2011). The goal of the UPR is to reduce the unfolded-protein load and promote ER protein folding capacity to restore balance. Folding capacity is promoted via increased expression of protein chaperones and other folding enzymes via IREα and ATF6 activation. There are four mammalian kinases activated during the ISR: heme-regulated eIF2α (HRI), double-stranded RNA-dependent protein kinase (PKR), general control non-depressible kinase 2 (GCN2), and PERK. Each kinase is activated by a specific cellular stressor and once activated, all phosphorylate serine 51 on the α-subunit of eIF2, resulting in SG formation, and ultimately, translational arrest. A schematic of this pathway is shown in Figure 2 (Appenzeller-Herzog, 2010). Long-term, low-dose BPA exposure can suppress later SG formation, which should be triggered by acute stressors, suggesting that chronic BPA exposure may impact a cell's ability to deal with environmental stress (Cui, Li, Ron, et al., 2011). It is theorized that this chronic BPA exposure and the resulting defect in later SG formation from acute stressors causes the adverse health effects observed in humans.

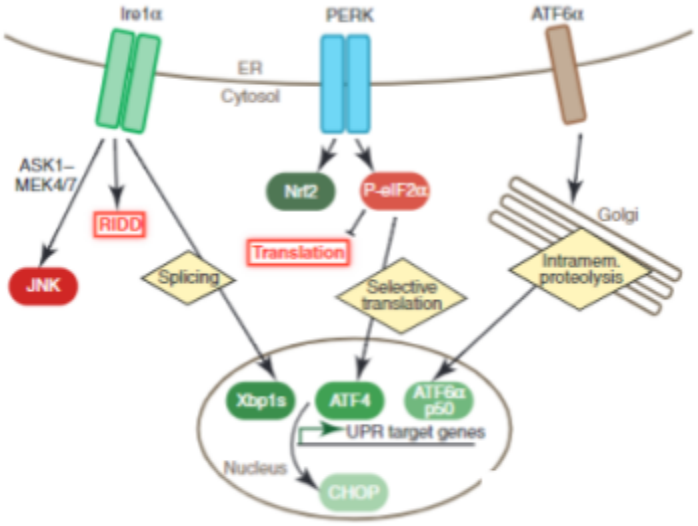

Figure 2. Ire1, PERK, and ATF6 pathway schematic. Reproduced from DeLeon, Wang, and Arnatt, 2020.

Overview of Estrogen Receptors

Estrogens, the primary female sex hormones, are steroid hormones responsible for female reproductive function and characteristics. Estrogens bind to extracellular estrogen receptors (ESRs) that ultimately control gene expression. There are several different types of estrogen receptors, the most classic of which are the nuclear receptors ESR1 (ER1/ERα) and ESR2 (ER2/ERβ) (Fuentes & Silveyra, 2019). Previous research has suggested that BPA-induced SG

formation does not function through either of these ESRs, although it is known that the PERK pathway is activated downstream (Friend, Hoppe, & Wu, 2018). The recently discovered G Protein-Coupled Estrogen Receptor (GPER1) is a membrane receptor that is responsible for mediating fast responses to estrogens via activation of extracellular signal-regulated kinases (ERKs) (Ho Vo, Hartig, Weinert, et al., 2019). Structurally, GPER1 contains 7 transmembrane α-helical domains, 4 extracellular domains, and 4 cytosolic domains. GPER1 shows low binding affinity for estrogen compared to ESR1 and ESR2. Because GPER1 is a membrane receptor, binding of estrogens to the extracellular domain triggers protein-kinase signaling cascades involving secondary messengers. There are 4 major cascades currently identified: phospholipase C (PLC)/protein kinase C (PKCs) pathway, Ras/Raf/MAPK cascade, phosphatidyl inositol 3 kinase (PI3K)/Akt kinase cascade, and cAMP/protein kinase A pathway.

Some mechanisms of crosstalk between genomic and nongenomic pathways have been described. For example, estrogen-bound nuclear estrogen receptors (ESR1 and ESR2) dimerize and translocate to the nucleus, where they bind phosphorylated transcription factors from the GPER1 pathway. Another mechanism involves interactions at the plasma membrane between GPER1 and these nuclear estrogen receptors, which activate protein kinase cascades that phosphorylate transcription factors, such as AP-1, STATs, and Elk-1, and nuclear estrogen receptors themselves. Figure 3 shows a diagram of these estrogen receptor pathways (Deleon et al., 2020).

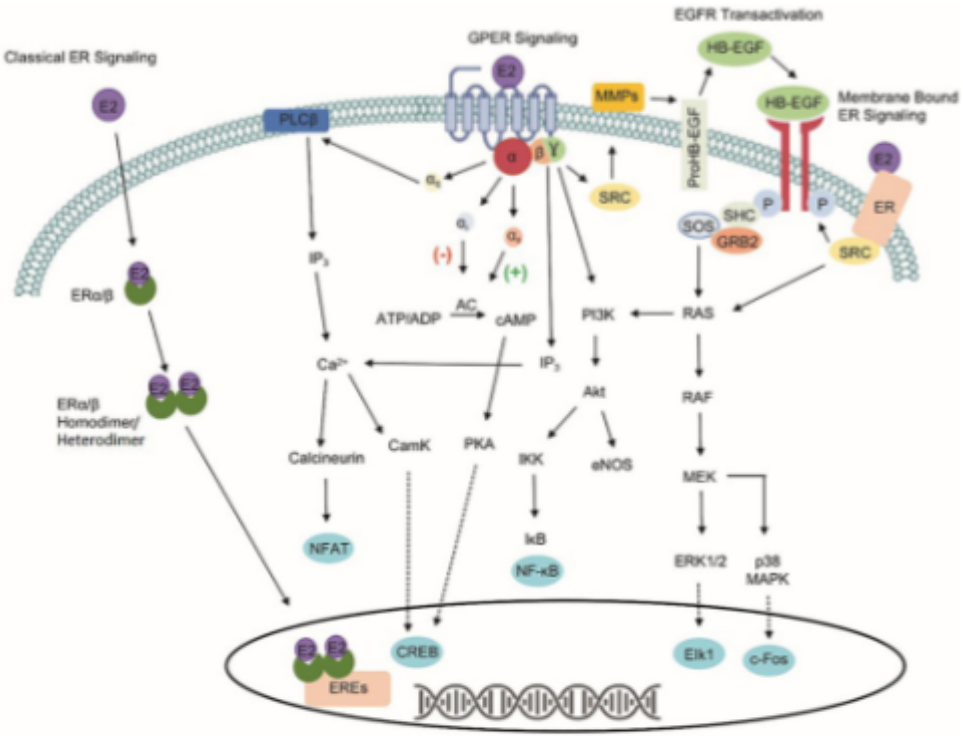

Figure 3. ESR1, ESR2, and GPER1 pathway crosstalk schematic. Reproduced from DeLeon, Wang, and Arnatt, 2020.

Activation of PERK via GPER1

Several studies have shown that the PERK pathway is activated downstream of GPER1 is several contexts, including cell proliferation, inflammation, and cholesterol gallstone formation (DeLeon, Wang, Gunn, et al., 2020; Notas, Panagiotopoulos, Vamvoukaki, et al., 2021; Xu, Wang, Wu, et al., 2017). While GPER1 has been identified as the mechanism through which PERK is activated in these contexts, it has yet to be explored in the context of stress granules. It has been previously noted that BPA-induced SGs form primarily through activation of the PERK pathway, suggesting that GPER1 may be involved in this process (Fay, Columbo, Cotter, et al., 2021). This project focuses on determining the pathway through which BPA triggers SG formation, with the hypothesis that BPA binds to GPER1, which activates the PERK pathway to induce SG formation.

GPER1 Agonists and Antagonists

Many GPER1 agonists and antagonists have been identified and utilized to research GPER1 activity; however, many of these drugs are not commercially available (DeLeon, Wang, & Arnatt, 2020). Of the agonists that are commercially available, such as the G-series GPER1 agonists, many are not GPER1 specific and exhibit cross-reactivity with the classic estrogen receptors ESR1 and ESR2 (DeLeon, Wang, & Arnatt, 2020). For the scope of this project, the GPER1 agonist G-1 was used as previous work has shown that ESR1 and ESR2 do not play a role in BPA-induced SG formation (Friend, Hoppe, & Wu, 2018). Of the antagonists that are commercially available, CIMBA is the only one that has been investigated in the literature due to its high specificity for GPER1 (DeLeon, Wang, & Arnatt, 2020).

Activation of GPER1 using the GPER1 agonist G-1 has been shown to activate the UPR in MCF-7 cells, as indicated by increased expression of the UPR markers PERK, ATF-4, GRP-78, and CHOP (Ho Vo, Hartig, Weinert, et al., 2019). In this pathway, shown in Figure 4, binding of G-1 to GPER1 results in ER Ca^{2+} efflux that triggers phosphorylation of PERK and IRE1α as well as cleavage of ATF6. This robust activation of GPER1 and the subsequent activation of the UPR via G-1 resulted in cell death in the estrogen receptor positive breast cancer cell line MCF-7 (Ho Vo, Hartig, Weinert, et al., 2019). The GPER1 antagonist CIMBA was used to protect against cholesterol gallstone

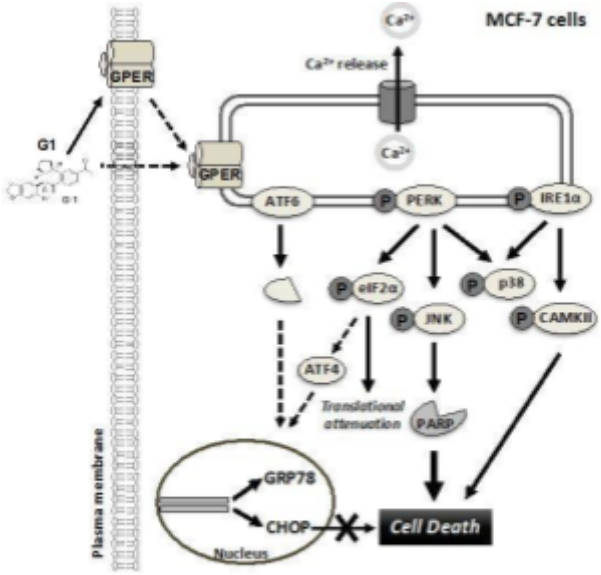

Figure 4. GPER1 signaling and activation of the cellular stress response. Reproduced from Ho Vo, Hartig, Weinert, et al., 2019.

formation in female mice by binding to and blocking activation of GPER1 (DeLeon, Wang, Gunn, et al., 2020).

Epidemiology of female reproductive cancers in NY state

In conjunction with my laboratory work, I conducted an epidemiological study on the incidence of female reproductive cancers in the state of NY in correlation with socioeconomic status as a marker of BPA exposure. I hypothesized that higher rates of breast, ovarian, and endometrial cancer would be correlated to low socioeconomic status due to increased exposure to BPA through canned food consumption. Newly diagnosed cancer cases in the state of NY reported from 2011-2015 were obtained from NY public health data ("Cancer Mapping," 2018). Data was formatted to display the three female reproductive cancers (FRCs) of interest: breast, ovarian, and uterine (endometrial). Observed cancer rates in each block group were compared to expected cancer rates for that block group and given a score of either 0 (expected was higher than or equal to observed) or 1 (observed was higher than or equal to expected). A composite score for each block group (0-3) was calculated by adding up the block group score for each FRC. The average composite score (0-3) for each county was calculated based on block group composite scores and compared to socioeconomic markers for each county. The socioeconomic markers used were students eligible for free lunch, food insecurity, and poverty, which were obtained from the USDA food assistance and insecurity data for the years in question ("Food Environment Atlas," 2022).

Chapter 2: Stressed Out! Role of GPER1 in BPA-Induced Stress Granule Formation

Background

This project focuses on determining the pathway through which BPA triggers SG formation, with the hypothesis that BPA binds to GPER1, which activates the PERK pathway to induce SG formation. Experiments were carried out on wild-type U2OS (wtU2OS) cells, which are a human osteosarcoma cancer cell line that shows moderate expression of GPER1. wtU2OS cells were obtained and cultured. Stress granule assays were conducted in 12 well plates containing sterile coverslips, to which cells were added and incubated overnight at 37 °C. Cells were then treated with 500 μM DMSO (negative control), 500 μM sodium arsenite (positive control), 250 μM BPA, 300 μM BPA, 400 μM BPA, and 500 μM BPA for one hour. Synergistic assays were also conducted in which cells were pretreated for 2 hours with either G-1 or CIMBA and then treated with either 250 μM BPA or 300 μM BPA. Cells were then fixed with PFA and methanol and treated with BSA. The primary rabbit antibody G3BP1 (1:1000) was used to directly bind SGs. The secondary rabbit antibody, which was tagged with a green fluorophore, was used to bind the primary antibody and indicate SGs while Hoescht, a blue nuclear dye, was used to visualize U2OS cells. Coverslips were mounted to microscope slides and analyzed for the presence of SGs via fluorescence microscopy.

Materials and Methods

Cell Culture

Wild-Type osteosarcoma (wtU2OS) cells were cultured in complete DMEM media (88% DMEM (+ glutamine, + glucose, - sodium pyruvate), 10% FBS, 1% Penicillin/Streptomycin, and 1% sodium pyruvate) and T75 flasks, which were replaced every 5 cell passages. Cells were incubated at 37°C with 5% CO_2 and sub-cultured every 1-3 days at a ratio of 1:2 or 1:4.

Acute Exposure Assay

wtU2OS cells were plated at a density of 1 x 10^5 cells/mL, 1 mL of media/well in 12-well plates containing coverslips. Plates were incubated overnight at 37°C. The following day, 0.5 mL of media from each well to receive the same treatment were combined and combined with their respective treatment: 500 µM DMSO (negative control), 500 µM sodium arsenite (positive control), 300 µM BPA, 400 µM BPA, or 500 µM BPA. Excess media was aspirated from the 12-well plates and 0.5 mL of treated media was returned to its respective well. Plates were incubated at 37°C for 1 hour.

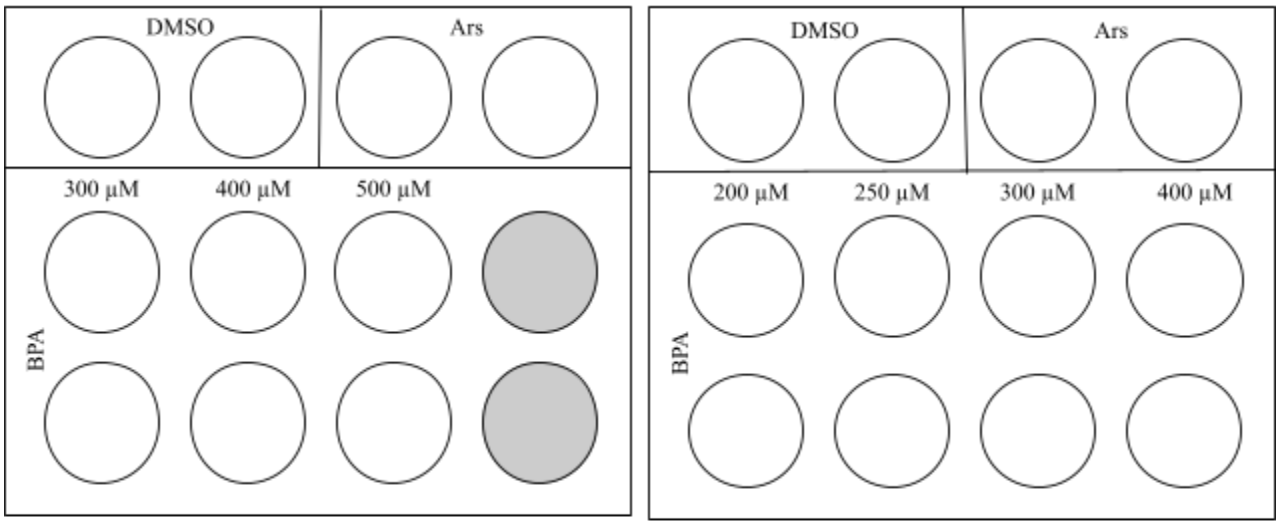

Figure 5. Acute Exposure Assay setup with treatments for each well. 500 µM DMSO was used as a negative control and 500 µM sodium arsenite (Ars) was used as a positive control. The following concentrations of BPA in DMSO were used: 200 µM, 250 µM, 300 µM, 400µM, and 500µM. Wells that were not used are grayed out.

Synergistic Exposure Assay

wtU2OS cells were plated at a density of 1 x 10^5 cells/mL, 1 mL of media/well in 12-well plates containing coverslips. Plates were incubated overnight at 37°C. The following day, 0.5 mL of media from each well to receive the same treatment were combined and combined with their respective treatment: 500 µM DMSO (negative control), 500 µM sodium arsenite (positive control), 250 µM BPA, 300 µM BPA, 1 µM G1, 1 µM CIMBA. Excess media was aspirated from the 12-well plates and 0.5 mL of treated media was returned to its respective well. DMSO,

sodium arsenite, and BPA wells were incubated for 1 hour at 37°C. Wells containing G1 and CIMBA alone were incubated for 2 hours at 37°C. Synergistic wells were pretreated for 2 hours with either G1 or CIMBA at 37°C then treated with BPA for 1 hour at 37°C.

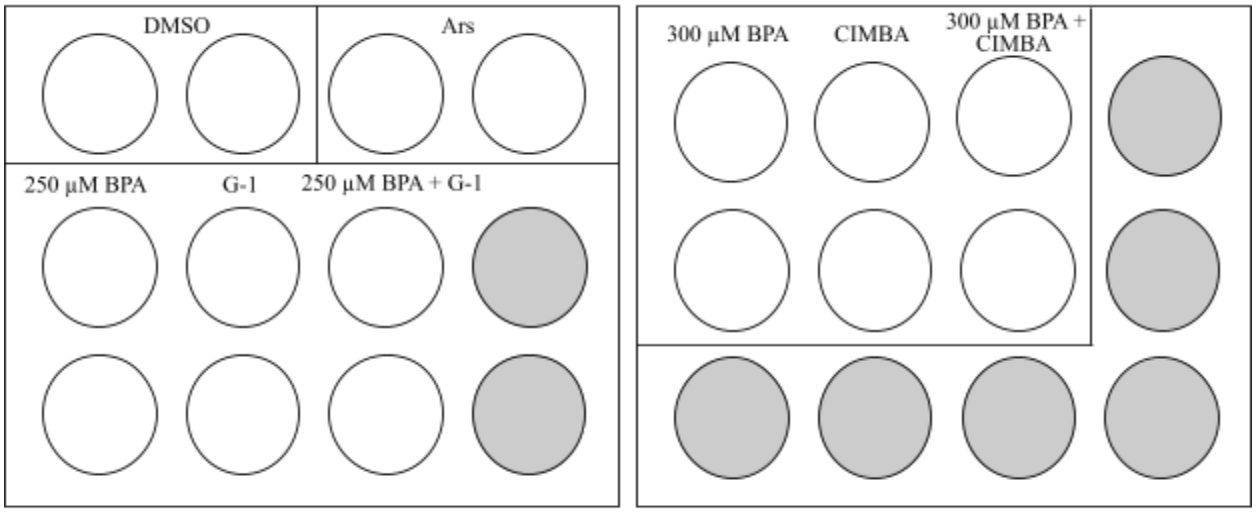

Figure 6. Synergistic Exposure Assay setup with treatments displayed for each well. 500 µM DMSO was used as a negative control and 500 µM sodium arsenite (Ars) was used as a positive control. Wells treated with 1 µM G1 and 1 µM CIMBA were incubated for 2 hours. Wells treated with both G1 and BPA or CIMBA and BPA were pretreated with their respective agonist/antagonist for 2 hours prior to BPA exposure. The following concentrations of BPA in DMSO were used: 250 µM and 300µM. Wells that were not used are grayed out.

G1/CIMBA Acute Exposure Assay

wtU2OS cells were plated at a density of 1 x 10^5 cells/mL, 1 mL of media/well in 12-well plates containing coverslips. Plates were incubated overnight at 37°C. The following day, 0.5 mL of media from each well to receive the same treatment were combined and combined with their respective treatment: 500 µM DMSO (negative control), 500 µM sodium arsenite (positive control), 1 µM G1, 10 µM G1, 100 µM G1, 1 µM CIMBA, 10 µM CIMBA, or 100 µM CIMBA. Excess media was aspirated from the 12-well plates and 0.5 mL of treated media was returned to its respective well. Plates were incubated at 37°C for 1 hour. 1 trial of this experiment was conducted as preliminary data for further experimentation.

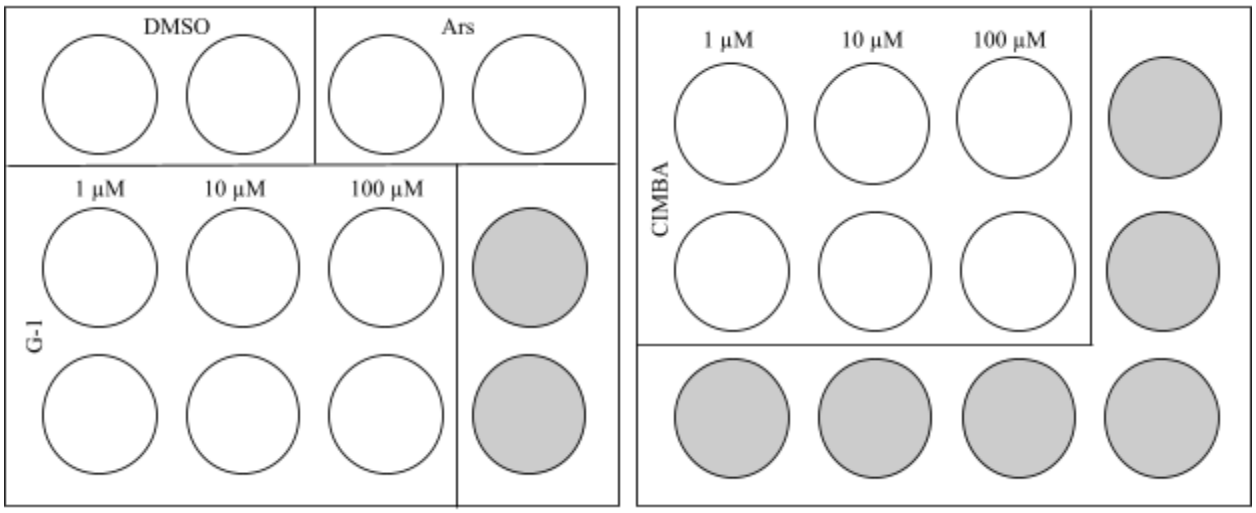

Figure 7. G1/CIMBA Acute Exposure Assay setup with treatments displayed for each well. 500 µM DMSO was used as a negative control and 500 µM sodium arsenite (Ars) was used as a positive control. The following concentrations of G1 and CIMBA in DMSO were used: 1 µM, 10 µM, and 100 µM. Wells that were not used are grayed out.

Cell Fixation and Blocking

Following the 1-hour incubation period, the wells were washed with non-sterile 1X PBS. Cells were fixed using 0.5 mL of 4% paraformaldehyde (PFA) and placed on the shaker at room temperature for 10 minutes. PSA was aspirated from all wells and replaced with 0.5 mL of non-sterile methanol (MeOH). Plates were placed on the shaker at room temperature for 10 minutes. Wells were washed 3 times with non-sterile 1X PBS. Cells were blocked using 0.5 mL of 5% BSA and placed on the shaker for 1 hour.

Antibody Staining

Following the incubation period, wells were washed with non-sterile 1X PBS. Cells were treated with 0.5 mL of the primary rabbit antibody for G3BP1 (1:1000) in 5% BSA and placed on the shaker for 1 hour. Wells were washed 3 times with non-sterile 1X PBS. Cells were treated with 0.5 mL of the secondary rabbit antibody tagged with a green fluorophore (1:500) and Hoescht (1:5000) in 5% BSA and placed on the shaker covered for 1 hour.

Mounting Slides

Secondary antibody mixture was aspirated from all wells. Slides were labeled appropriately and small drops of vinol were placed where the coverslips would be mounted. Coverslips were carefully removed from their respective wells using forceps and placed top down on the vinol drop. Coverslips were pressed down evenly and excess vinol was removed using water and Kim wipes. Slides were stored in a slide deck to prevent photobleaching.

Data Collection and Statistical Analysis

Slides blinded using tape to hide the slide label containing the treatment then re-labelled with a letter. were scored based on the percentage of cells containing SGs in a single-blind manner. At least 250 cells in at least 3 views were scored and cell counts were used to calculate the percentage of SG formation for each treatment. Experiments were repeated for a total of 3 trials, unless otherwise indicated.

Results

Initial Acute Exposure Assays were conducted with various concentrations of BPA in DMSO to determine the concentrations that would be used to measure the effects of G1 and CIMBA on SG formation. The results of these trials are shown in Figure 8. To first determine the optimal BPA concentration that would later be used to explore the effects of the GPER1 agonist and antagonist, an Acute Exposure Assay was performed. The goal of this experiment was to identify a BPA concentration that reliably produced ~50% SG formation such that increases and decreases in SG formation caused by the GPER1 agonist and antagonist could be observed. wtU2OS cells were therefore treated with concentrations of BPA ranging from 200-500 µM. The results are shown in Figure 8.

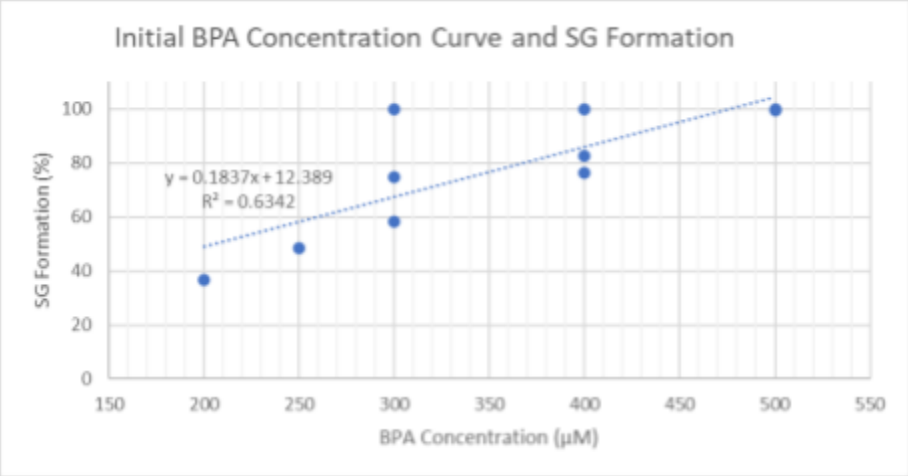

Figure 8. Scatter Plot of Initial BPA Concentrations with line of best fit. BPA was dissolved in DMSO and concentrations ranged from 200 µM to 500 µM. Cells were treated with BPA for 1 hour at 37°C. Line of Best Fit: $y = 0.1837x + 12.389$. $R^2 = 0.6342$.

As G1 was hypothesized to increase SG formation due to activation of GPER1, 250 µM BPA was chosen as the treatment concentration as it was found to trigger ~ 50% SG formation in the Acute Exposure Assays, which allowed for shifting in either direction to be detected. As CIMBA was hypothesized to decrease SG formation through blocking of GPER1 activation, 300 µM BPA was chosen as the treatment concentration as it was found to trigger ~77% SG formation in the Acute Exposure Assays, which allowed more room for detection of decreased SG formation.

The Synergistic Exposure Assay involved pre-treating cells for 2 hours with either G1 or CIMBA followed by a 1 hour treatment with BPA and observing the percentage of SG formation. Each treatment and pre-treatment were also scored to determine baseline values for SG formation.

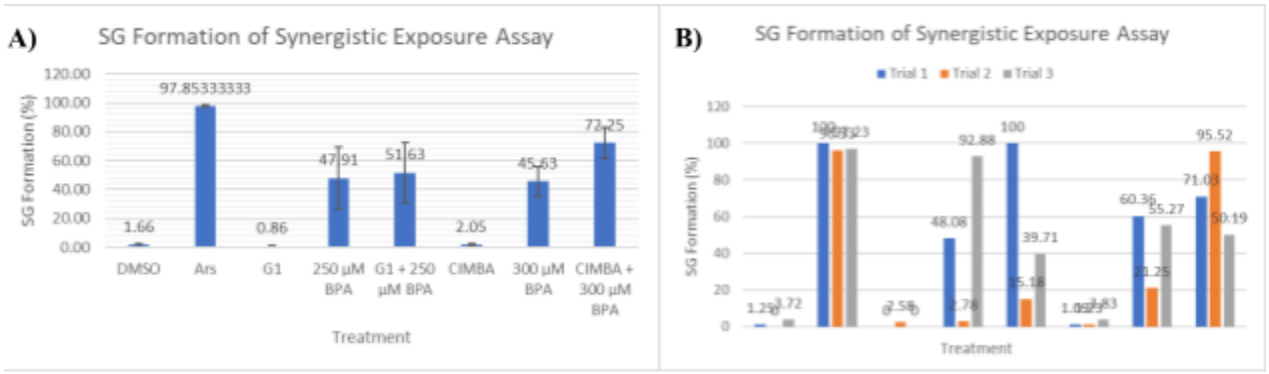

Figure 9. Bar Graph of Synergistic Exposure Assay results with standard error bars and individual trial results.

As shown in Figure 9, pretreatment with G1 and CIMBA followed by treatment with BPA did not produce a significant change in SG formation, as confirmed by T-Test. DMSO (negative control), G1, and CIMBA all showed no significant SG formation, suggesting that any changes in SG formation with pretreatments was due to synergy. Ars (positive control) was found to produce ~ 100% SG formation at 500 µM. Cell images from the Synergistic Exposure Assay are shown in Figure 10.

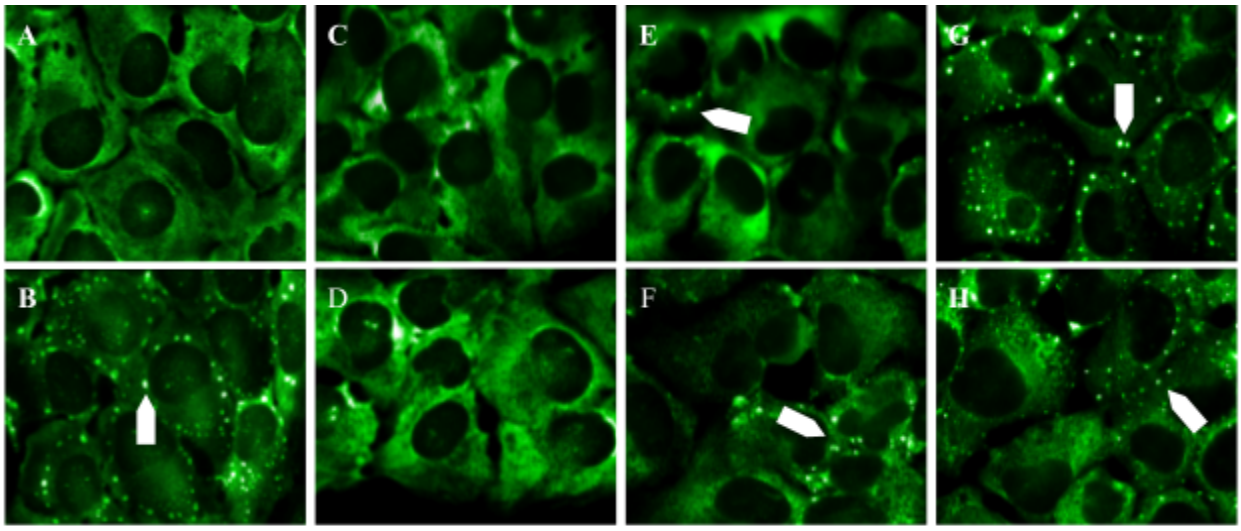

Figure 10. Fluorescence Microscopy snapshots of cells from trial 1 of the Synergistic Exposure Assay. A) DMSO. B) sodium arsenite. C) G1 alone. D) CIMBA alone. E) 250 µM BPA. F) 300 µM BPA. G) G1 + 250 µM BPA. H) CIMBA + 300 µM BPA. White arrows indicate stress granules.

To determine if G1 and CIMBA cause SG formation at higher concentrations, one trial of a Dose Curve Assay was conducted with the following G1 and CIMBA concentrations: 1 µM, 10 µM, and 100 µM. The results are shown in Figure 11. These results suggest that at high concentrations G1 may be sufficient to cause SG formation on its own and CIMBA is not sufficient to cause SG formation, as is consistent with the hypothesis.

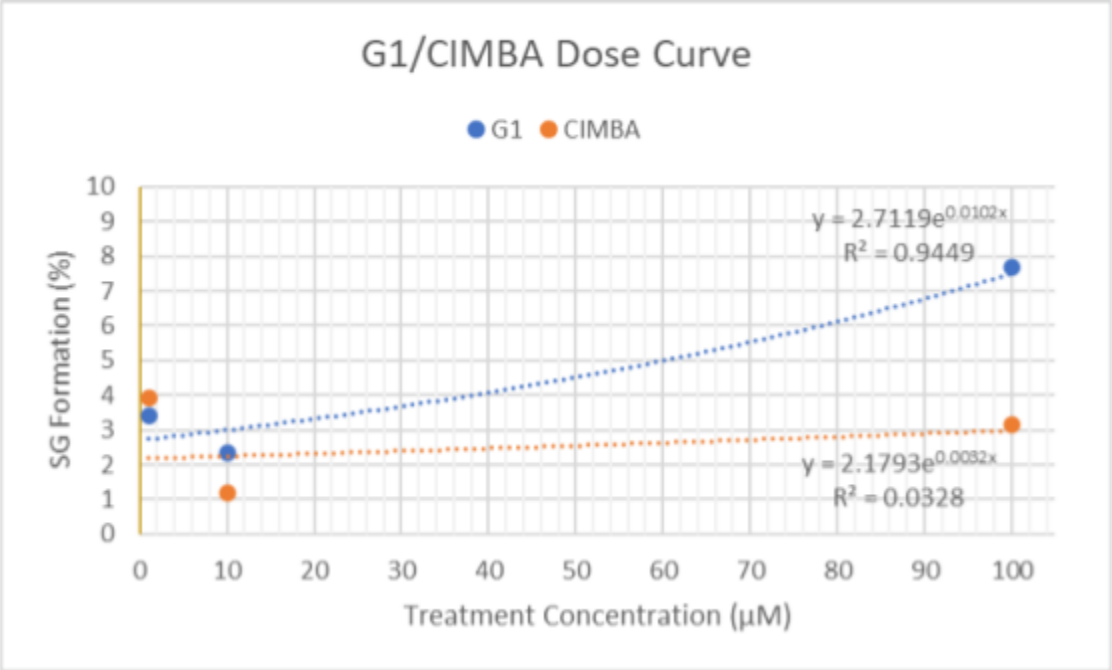

Figure 11. Scatter Plot of G1 and CIMBA Dose curve with line of best fit and R^2 value for each data set. G1: $y = 2.7119e^{0.0102x}$, $R^2 = 0.9449$. CIMBA: $y = 2.1793e^{0.0032x}$, $R^2 = 0.0328$.

Conclusions

As shown in Figure 8, the initial BPA concentration curve followed a linear distribution with a line of best fit slope of $y = 0.1837x + 12.389$ and R^2 value of 0.6342. The greatest variance between trials of this experiment was seen in 300 μM BPA, which produced 58-100% SG formation. This data suggests that 300 μM BPA approaches the concentration threshold for SG formation and that the inherent error of micropipettes was enough to produce these variable results. 300 μM BPA was used in conjunction with CIMBA in the Synergistic Exposure Assay. 250 μM BPA, which produced 48.34% SG formation, was used in conjunction with G1 in the Synergistic Exposure Assay.

As shown in Figure 9, the Synergistic Exposure Assay produced highly variable results. A statistically significant difference in SG formation was found between the positive (ars) and negative (DMSO) controls, as confirmed by a paired T-Test ($p = 5.96 \times 10^{-5}$). No statistically significant difference was found between BPA + G1/CIMBA synergy and treatment with BPA alone ($p = 0.22$), although trials 1 and 2 of the Synergistic Exposure Assay both showed an ~50% increase in SG formation. Lack of literature citing the use of G1 and CIMBA to study SGs may account for the obtained results as pretreatment doses may have been suboptimal, especially for CIMBA, which has only been used in 1 published study to date. Neither G1 nor CIMBA produced any significant SG formation at the 1 μM concentrations used in the Synergistic Exposure Assays, suggesting that any change in SG formation seen in synergy treatments can be attributed to synergy between G1/CIMBA and BPA.

Trial 1, representative images are shown in Figure 10, showed the most promising results with SG formation increasing from 48% with 250 μM BPA alone, which was consistent with the BPA concentration curve produced from the Acute Exposure Assays, to 100% with 250 μM BPA and G1 synergy. Trial 1 showed no statistically significant difference between SG formation from 300 μM BPA alone (60%) and 300 μM BPA and CIMBA synergy (71%), reinforcing the notion that the agonist and antagonist concentrations should be optimized for further experiments. Additionally, the size of the SGs also seemed to differ between BPA treatment alone and synergy. For example, SG size appeared to increase between 250 μM BPA alone (Panel E) to 250 μM BPA and G1 pretreatment (Panel G), suggesting that pretreatment with G1 not only increased the number of cells that produced SGs but also the size of the SGs produced. Additionally, SG size appeared to decrease between 300 μM BPA alone (Panel F) to 300 μM BPA and CIMBA pretreatment (Panel H), suggesting that although pretreatment with CIMBA did not show any statistical difference in the number of cells that produced SGs, appeared to decrease the size of the SGs produced. Both of these findings are consistent with the hypothesis that GPER1 modulates BPA-induced SG formation and marks an additional area for quantification of BPA-induced cellular stress. These findings will need to be quantified and validated by measuring SG diameter and area using digital image analysis software such as Zen or ImageJ.

As shown in Figure 11, G1 produced a slight increase in SG formation at higher concentrations, following an exponential line of the best fit with a slope of $y = 2.7119 \times 10^{0.0102x}$

and R^2 value of 0.9449, suggesting high correlation. This finding suggests that at high concentrations G1 may be sufficient to activate the ISR and trigger SG formation, as is consistent with the hypothesis. CIMBA did not appear to produce SGs even at higher concentrations, following a linear line of best fit with a slope of $y = 2.1793 \times 10^{0.0032x}$ and R^2 value of 0.0328, suggesting poor correlation. No statistically significant difference in SG formation between any of the G1 or CIMBA doses. This finding suggests that even at high concentrations, CIMBA alone is not sufficient to activate the ISR and trigger SG formation, as is consistent with the hypothesis.

Limitations

Due to limited time, few replicates were produced for the given experiments. More replicates of the assays should be performed to explore the relationship between GPER1 and BPA-induced SG formation. Higher concentrations of CIMBA should be considered for Synergistic Exposure Assays as the hypothesized result was not observed, likely due to suboptimal drug concentrations.

Further Research

Additional replicates of the Synergistic Exposure Assay should be conducted to more clearly determine the effect of synergy on SG formation. Higher pretreatment concentrations of CIMBA should also be considered to optimize this protocol. The G1/CIMBA Acute Exposure Assay should also be repeated with concentrations of G1 more closely resembling that of BPA (e.g. 200-500 μM) to confirm that G1 is sufficient to trigger SG formation at higher concentrations. GPER1 knockout cell lines could also be engineered to determine the effects on SG formation in response to BPA. Finally, the size and number of SGs in individual cells could also be quantified to capture the more subtle changes in SG formation produced from GPER1 modulation.

Chapter 3: Incidence of Female Reproductive Cancers in Correlation with Socioeconomic Status in NY State as a Marker of BPA Exposure

Background

I conducted an epidemiological study of the incidence of female reproductive cancers in the state of NY in correlation with socioeconomic status as a marker of BPA exposure. I hypothesized that higher rates of breast, ovarian, and endometrial cancer would be correlated to low socioeconomic status due to increased exposure to BPA through canned food consumption.

Exposure to BPA and bisphenol analogues is correlated to endocrine disruption and, subsequently, estrogen-related cancers such as breast, ovarian, and endometrial. Ingestion of food that has been in contact with BPA and bisphenol analogues is believed to have the greatest exposure risk, as compared to dermal contact and spatial proximity. BPA and, more recently bisphenol analogues, have been used for the manufacture of food cans.

Due to decreased price of canned foods compared to fresh foods, increased shelf life and therefore ability to buy in bulk, and increased availability in food deserts, factors that often affect those in poverty, it is predicted that low socioeconomic status may be correlated with breast, ovarian, and endometrial cancer.

Materials and Methods

Obtaining Patient Data

Newly diagnosed cancer cases in the state of NY reported from 2011-2015 were obtained from NY public health data ("Cancer Mapping," 2018). Data was formatted to display the three female reproductive cancers (FRCs) of interest: breast, ovarian, and uterine (endometrial). Observed cancer rates in each block group were compared to expected cancer rates for that block group and given a score of either 0 (expected was higher than or equal to observed) or 1 (observed was higher than or equal to expected). A composite score for each block group (0-3) was calculated by adding up the block group score for each FRC. The average composite score (0-3) for each county was calculated based on block group composite scores and compared to socioeconomic markers for each county. The socioeconomic markers used were the proportion of students eligible for free lunch and the proportion of people living below the poverty line, which were obtained from the USDA food assistance and insecurity data for the years in question ("Food Environment Atlas," 2022). A pre-made ArcGIS map containing points for each healthcare facility in the state of NY was obtained from NY public health data ("Health Facility Map," 2023).

Data Analysis

Average scores for each female reproductive cancer (breast, ovarian , and uterine) composite score for FRCs, proportion of students eligible for free lunch, and proportion of people living below the poverty line in each county were used to calculate standard deviation (SD), interquartile range (IQR), upper limit for outliers, and lower limit for outliers for each marker. Data was conditionally formatted to highlight cells within one SD above and below the mean, greater than one SD above or below the mean, and outliers above the upper limit or below the lower limit. Counties that included one or more outlier in the poverty markers or composite FRC score were excluded from analysis.

Statistical Tests

The statistics coding program 'R' was used to run statistical analysis on the formatted data. Normal Q-Q plots relating the breast, ovarian, uterine, and combined FRC scores individually to poverty rate and percentage of students eligible for free lunch were generated. ANOVA Tests were ran on the breast, ovarian, uterine, and combined FRC scores individually with poverty rate and percentage of students eligible for free lunch to determine statistical significance of the data. Finally, Pearson's Correlation Tests were run on the breast, ovarian, uterine, and combined FRC scores individually to poverty rate and percentage of students eligible for free lunch to determine the degree of correlation between each cancer marker and the poverty markers.

Results

County	FRC Score	Free Lunch	Poverty Rate
Albany	1.490	0.297	0.126
Allegany	1.475	0.365	0.168
Bronx	1.132	0.783	0.303
Broome	1.428	0.316	0.177
Cattaraugus	1.458	0.332	0.180
Cayuga	1.057	0.277	0.127
Chautauqua	1.348	0.372	0.172
Chemung	1.266	0.358	0.175
Chenango	1.489	0.371	0.143
Clinton	1.304	0.291	0.175
Columbia	1.00	0.277	0.136
Cortland	1.558	0.303	0.162
Delaware	1.377	0.355	0.169
Dutchess	1.383	0.195	0.104
Erie	1.419	0.346	0.156
Essex	1.229	0.288	0.122
Franklin	0.861	0.363	0.183
Fulton	1.283	0.344	0.179
Genesee	1.538	0.263	0.134
Greene	1.333	0.257	0.164
Hamilton	1.500	0.170	0.111
Herkimer	1.197	0.321	0.127
Jefferson	1.192	0.311	0.141
Kings	1.198	0.689	0.223
Lewis	1.182	0.297	0.140
Livingston	1.233	0.224	0.132
Madison	1.149	0.270	0.129
Monroe	1.274	0.345	0.148
Montgomery	1.238	0.329	0.184
Nassau	1.398	0.146	0.061
New York	1.348	0.631	0.176
Niagara	1.354	0.309	0.155
Oneida	1.365	0.362	0.180
Onondaga	1.344	0.320	0.146
Ontario	1.346	0.201	0.096
Orange	1.258	0.265	0.121
Orleans	1.267	0.335	0.142
Oswego	1.430	0.3451	0.174
Otsego	1.549	0.271	0.168
Putnam	1.463	0.066	0.060
Queens	1.156	0.608	0.139
Rensselaer	1.234	0.266	0.120
Richmond	1.414	0.449	0.142
Rockland	1.371	0.208	0.140
St. Lawrence	1.108	0.350	0.185
Saratoga	1.374	0.119	0.064
Schenectady	1.361	0.307	0.120
Schoharie	1.357	0.269	0.137
Schuyler	0.889	0.270	0.125
Seneca	1.000	0.283	0.141
Steuben	1.102	0.346	0.154
Suffolk	1.429	0.185	0.078
Sullivan	1.229	0.358	0.181
Tioga	1.222	0.307	0.117
Tompkins	1.444	0.281	0.201
Ulster	1.280	0.254	0.140
Warren	1.277	0.221	0.113
Washington	1.333	0.287	0.133
Wayne	1.557	0.279	0.122
Westchester	1.366	0.258	0.101
Wyoming	1.524	0.234	0.133
Yates	1.381	0.363	0.136
NY State	1.310	0.314	0.145

Table 1. Female Reproduce Cancer Score (FRC Score), proportion of students eligible for free lunch (Free Lunch), and proportion of individuals below the poverty line (Poverty Rate) for each county in NY state.

The calculated breast, ovarian, uterine, and combined FRC scores for each county were compared to the proportion of students eligible for free lunch (Free Lunch) and proportion of individuals living below the poverty line (Poverty). These data were compared to the calculated means for the state of NY and ANOVA tests were conducted to test for statistical significance. First, Normal Q-Q plots were generated for each individual FRC and the combined FRC separately against the combined poverty markers to determine the distribution of the data. All Normal Q-Q plots displayed linear outputs, confirming that the data followed a normal distribution. Figure 12 shows the Normal Q-Q plot for Breast Cancer.

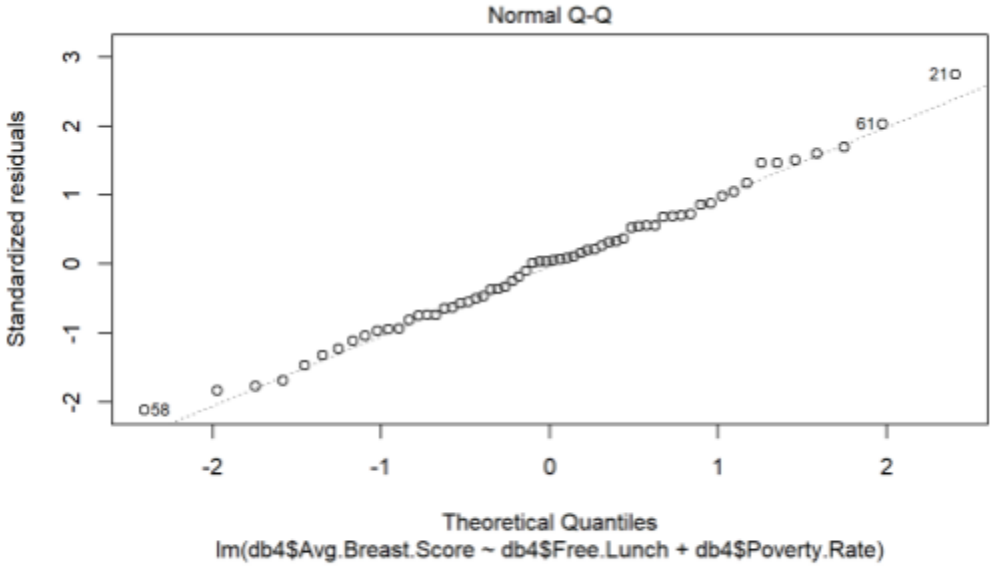

Figure 12. Normal Q-Q Plot of Breast Score against the poverty markers Free Lunch and Poverty Rate. Graph was generated from the formatted NY State health data using R.

Since the data was shown to have a normal distribution, two-tailed ANOVA Tests were conducted on each of the individual FRC scores and combined FRC score against the poverty markers to test how, in combination, they affect each cancer score. Overall, these tests reject the null hypothesis that there is no correlation between FRCs and poverty and accept the hypothesis that there is a correlation between FRCs and poverty in NY state using a 95% confidence interval P Value < 0.05). Figure 13 shows the code and value outputs for the ANOVA Tests,

```
> anova(lm(db4$Avg.Breast.Score~db4$Free.Lunch+db4$Poverty.Rate))
Analysis of Variance Table

Response: db4$Avg.Breast.Score
                 Df  Sum Sq  Mean Sq F value   Pr(>F)
db4$Free.Lunch    1 0.07896 0.078962  9.8962 0.002595 **
db4$Poverty.Rate  1 0.00409 0.004089  0.5125 0.476880
Residuals        59 0.47076 0.007979
---
Signif. codes:
0 '***' 0.001 '**' 0.01 '*' 0.05 '.' 0.1 ' ' 1

> anova(lm(db4$Avg.Ovary.Score~db4$Free.Lunch+db4$Poverty.Rate))
Analysis of Variance Table

Response: db4$Avg.Ovary.Score
                 Df  Sum Sq   Mean Sq F value Pr(>F)
db4$Free.Lunch    1 0.00007 0.0000660  0.0110 0.9166
db4$Poverty.Rate  1 0.00309 0.0030945  0.5178 0.4746
Residuals        59 0.35258 0.0059760

> anova(lm(db4$Avg.FRC.Score~db4$Free.Lunch+db4$Poverty.Rate))
Analysis of Variance Table

Response: db4$Avg.FRC.Score
                 Df  Sum Sq  Mean Sq F value  Pr(>F)
db4$Free.Lunch    1 0.07959 0.079591  3.3261 0.07325 .
db4$Poverty.Rate  1 0.00022 0.000219  0.0092 0.92407
Residuals        59 1.41181 0.023929
---
Signif. codes:  0 '***' 0.001 '**' 0.01 '*' 0.05 '.' 0.1 ' ' 1
```

Figure 13. ANOVA Test results for each individual FRC and combined FRC against the poverty markers

The ANOVA Tests established that there was a statistical correlation between FRCs and poverty, but the type of relationship between these variables was not yet known. To examine this relationship, FRC scores and poverty marker values were examined together on a county-by-county basis to determine whether they supported the hypothesis or not. Counties that contained an FRC and at least one poverty marker that agreed (both higher or lower than the population mean) were considered to support the hypothesis that higher rates of FRCs correlate to low socioeconomic status. Counties that contained an FRC and two poverty markers that disagreed (one higher and the other lower than the population mean) were considered to reject the hypothesis. Counties that contained outliers in the FRC and/or one or more poverty markers were excluded from analysis. Of the 62 counties in NY state, 36 supported the hypothesis (58.07%), 23 rejected the hypothesis (37.10%), and 3 were outliers (4.839%). Figure 14 shows a map visually displaying these results.

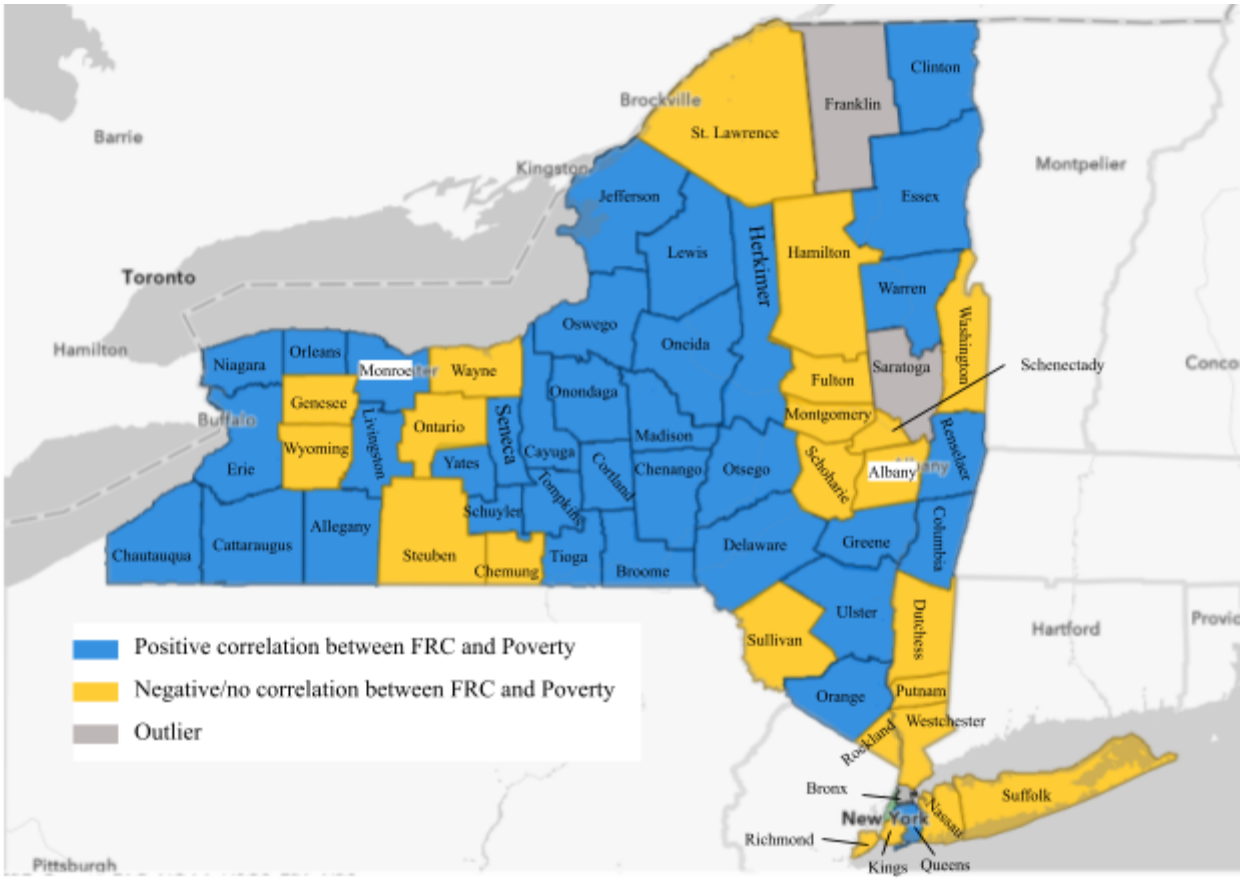

Figure 14. Color-Coded Map of NY State according to the FRC and Poverty Marker correlation findings.

In order to examine some of the confounding variables that may be at play, access to diagnostic healthcare was assessed by overlaying a map of healthcare facilities in the state of NY to the map generated above ("Healthcare Facility Map," 2023). Additionally, Healthcare Density was calculated based on this value and Population Density was obtained for the year 2015. Figure 15 depicts the map overlay while Table 2 shows the healthcare and population data.

County	Healthcare Density	Population Density
Albany	0.008	591.780
Allegany	0.002	46.110
Bronx	0.261	34571.120
Broome	0.004	278.510
Cattaraugus	0.002	59.560
Cayuga	0.001	113.200
Chautauqua	0.005	123.350
Chemung	0.005	213.750
Chenango	0.001	54.660
Clinton	0.001	78.290
Columbia	0.002	96.910
Cortland	0.002	97.230
Delaware	0.003	31.930
Dutchess	0.004	371.720
Erie	0.012	884.810
Essex	0.013	21.450
Franklin	0.001	31.100
Fulton	0.002	108.970
Genesee	0.002	119.560
Greene	0.	73.590
Hamilton	0	2.740

County	Healthcare Density	Population per Capita
Herkimer	0.001	44.710
Jefferson	0.002	92.730
Kings	0.212	21.150
Lewis	0.001	102.440
Livingston	0.002	109.720
Madison	0.003	1140.580
Monroe	0.011	123.170
Montgomery	0.005	123.170
Nassau	0.039	4781.360
New York	0.964	107.100
Niagara	0.010	191.760
Oneida	0.003	601.840
Onondaga	0.006	170.110
Ontario	0.005	465.260
Orange	0.007	106.280
Orleans	0.003	126.250
Oswego	0.003	60.530
Otsego	0.002	430.040
Putnam	0.004	245.640
Queens	0.092	21553.030
Rensselaer	0.003	245.640

County	Healthcare Density	Population Density
Richmond	0.086	8130.170
Rockland	0.023	1878.630
St. Lawrence	0.002	41.410
Saratoga	0.001	279.330
Schenectady	0.020	755.940
Schoharie	0.002	50.380
Schuyler	0.003	55.390
Seneca	0	107.610
Steuben	0.003	70.210
Suffolk	0.012	1646.390
Sullivan	0.002	77.340
Tioga	0	95.360
Tompkins	0.002	221.060
Ulster	0.002	160.240
Warren	0.001	74.620
Washington	0	74.870
Wayne	0.002	151.440
Westchester	0.014	2268.050
Wyoming	0.002	69.190
Yates	0.003	74.080
NY State	0.005	420.060

Table 2. Healthcare Density (healthcare facilities per square mile) and Population Density (people per square mile) for each county in NY state. Cells are color-coded according to the correlation between FRC and Poverty.

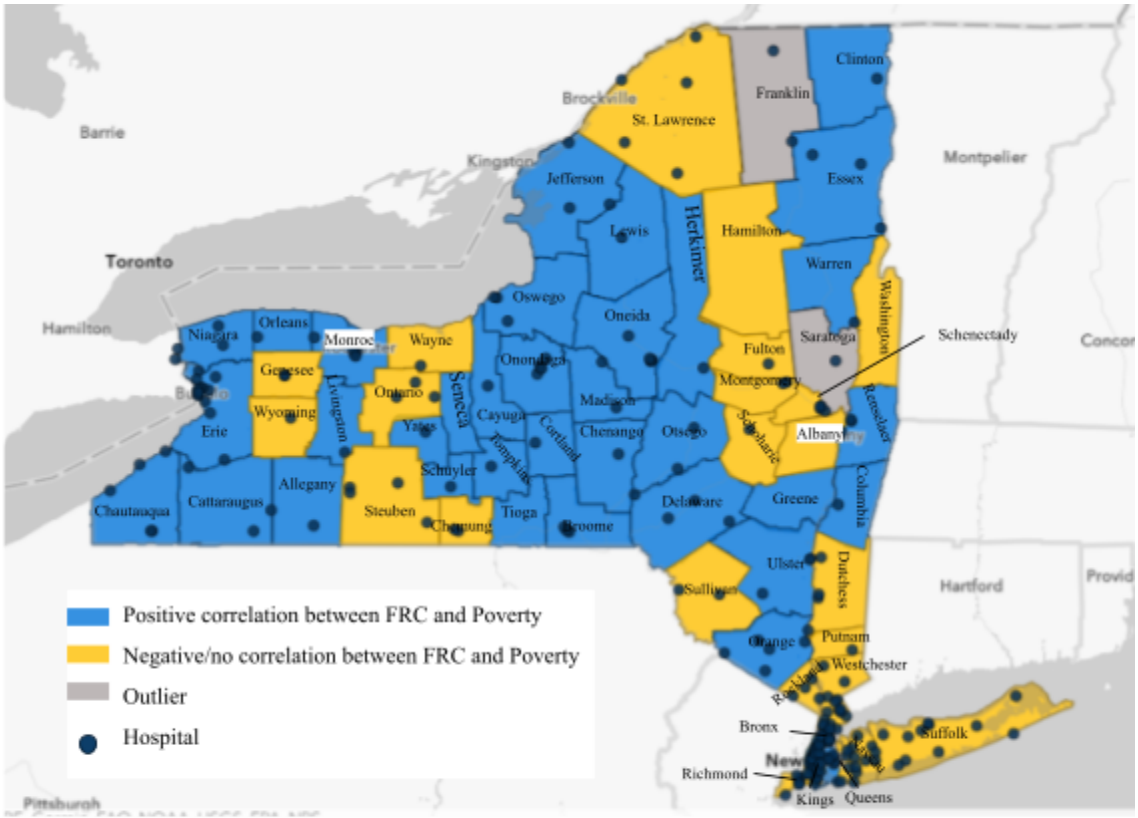

Figure 15. Color-Coded Map of NY State according to the FRC and Poverty Marker correlation findings overlayed with points marking the locations of hospitals.

Conclusions

As shown in Figure 14, 36 counties supported the hypothesis (58.07%), 23 rejected the hypothesis (37.10%), and 3 were outliers (4.839%). These results are statistically significant, suggesting that there is a correlation between FRCs and poverty.

Limitations

This study relies on the assumption that individuals living in poverty consume more canned foods than those living above the poverty line, something that has yet to be concretely studied. Additionally, there are several confounding variables complexing the relationship between cancer and socioeconomic status, including but not limited to access to healthcare, degree of urbanization, and workplace exposures.

Healthcare Disparities

Figure 15 addressed access to healthcare, which can result in decreased diagnostic rates and preventative care in populations lacking access to healthcare. For example, many of the counties in the northeastern portion of the state that did not show a positive correlation between FRCs and poverty have fewer healthcare facilities within the county, which may account for this finding. For example, St. Lawrence and Fulton both show low rates of FRCs and high rates of poverty with low Healthcare Density and Population Density, suggesting that these counties are rural with limited access to healthcare and therefore less likely to obtain a cancer diagnosis. Similarly, Schenectady showed high rates of FRC and low poverty with high Healthcare Density and high Population Density, suggesting that individuals residing in this county have greater access to healthcare and therefore are more likely to obtain a cancer diagnosis compared to more rural counties. Hamilton on the other hand showed high rates of FRC and low rates of poverty with no healthcare facilities and very low population density, suggesting that other confounding variables may also be at play.

Outliers

By definition, 3 counties were considered to be statistical outliers: Franklin, Saratoga, and Bronx. Franklin was considered an outlier due to its unusually low uterine and combined FRC scores. After additional analysis, Franklin was also found to have a low population density and healthcare density. These findings suggest that this county is very rural and lacks access to healthcare and therefore diagnostic capabilities. Saratoga was considered an outlier due to its unusually low proportion of students eligible for free lunch. Paired with low poverty rate and high rates of FRC, it would be expected that Saratoga would have high Healthcare Density; however, both the Healthcare Density and Population Density are low for the county. Additional research revealed that General Electric dumped over a million pounds of polychlorinated biphenyls (PCBs), a known carcinogen, in the Hudson River from 1947-1977. This environmental risk and toxic exposure is likely to have had the greatest effect on individuals residing in Saratoga, Albany, Rensselaer, Greene, Columbia, Ulster, and Dutchess counties

(“PCBs and Human Health,” n.d.”). This may have contributed to the high rates of FRC observed in these counties.

Finally, Bronx was considered an outlier due to its unusually high values of Free Lunch and Poverty Rate. Bronx has the greatest Population Density of any county paired with high Healthcare Density. The healthcare disparity in this county, marked by the large socioeconomic disparity in the region, may account for the low rates of FRC as the individuals living in poverty may lack the means to obtain healthcare, including transportation, financial support, and knowledge of resources. On the upper end of this disparity, individuals from wealthier backgrounds, while having access to the diagnostic capabilities of healthcare may also reap the benefits of preventative care, as is reflected in the low rates of FRC in Bronx. A similar trend was seen across Long Island, suggesting that healthcare disparity may be diffuse throughout the region, accounting for the observed results.

Chapter 4: Discussion

Discussion

As described in Chapter 2, the obtained findings were consistent with the hypothesis that GPER1 modulates BPA-induced SG formation. Figure 16 depicts a schematic with the proposed pathway of BPA-induced SG formation based on the literature and experimental results obtained in this study. This schematic proposes that BPA interacts with GPER1, causing it to translocate from the plasma membrane to that of the endoplasmic reticulum, where it phosphorylates and activates PERK. As has been confirmed in prior studies, PERK then phosphorylates eIF2α, which shuts down the translation and causes the transcription factor ATF4 to promote transcription of UPR target genes geared toward conservation of cellular energy and formation of SGs to relieve the unfolded protein load.

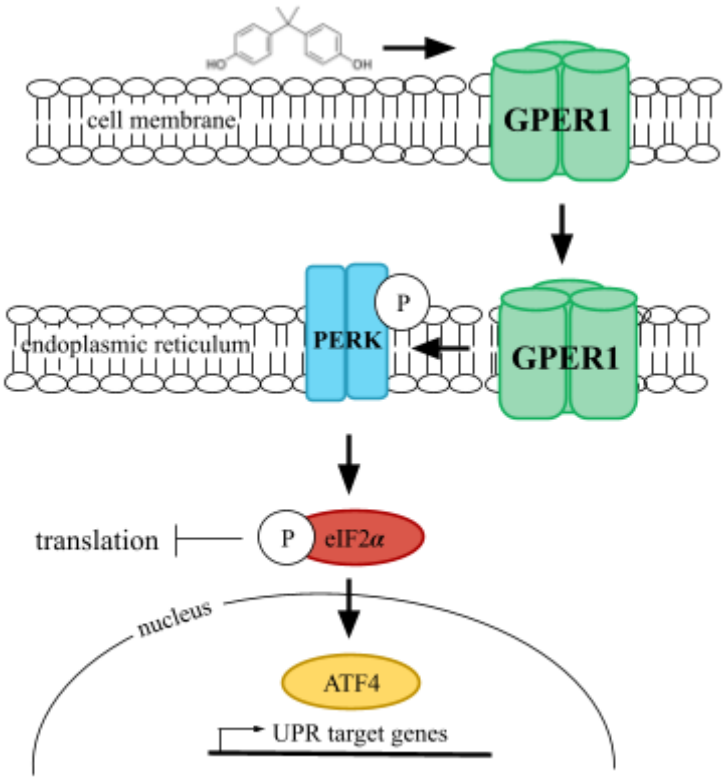

Figure 16. Proposed schematic of GPER1 modulation of BPA-induced SGs

BPA and Public Health

BPA has been identified as a potential endocrine disruptor and is associated with many disease states, such as endocrine-dependent cancers, infertility, and Polycystic Ovarian Syndrome (PCOS). Chronic exposure to BPA and the associated adverse health effects may be related to the assembly of SGs and altered induction of the integrated stress response (ISR) in subsequent exposures to cellular stressors. Determining the pathway through which BPA-induced SGs are

formed can provide immense insight into potential therapeutics to combat BPA-induced SG formation and lower disease risk.

Cancer Risk and Socioeconomic Status

The epidemiological study presented in Chapter 3 found a positive relationship between FRCs and socioeconomic status. In this study, this correlation was attributed to BPA exposure through canned food consumption, which was assumed to be related to socioeconomic status. While the results obtained seem to support the hypothesis, several confounding variables also related to socioeconomic status exist. These confounding variables are likely to produce similar findings in additional studies relating cancer rates to socioeconomic status. For example, occupational exposures to asbestos are a risk factor for development of mesothelioma, a rare lung cancer ("Mesothelioma," n.d.). Additionally, environmental exposure to carcinogens, such as exposure to PCB in the Hudson River Valley described above, may also affect cancer risk. Here lies a fundamental question in public health research: why do individuals participate in activities and/or live in areas that increase their exposure risks?

There are several factors that contribute to individuals exposing themselves to carcinogens, such as financial restraints, affinity characteristics, and lack of public knowledge. In the case of ingesting canned foods, financial restraints, lack of access to fresh foods, and lack of public knowledge are the predominant motivators for continued canned food consumption. Canned foods are less expensive compared to fresh foods, non-perishable, and widely available, making them an easy alternative to both fresh and frozen foods. Aside from personal use of canned foods, food banks also primarily serve canned foods to their guests both due to reduced cost and shelf stability. Both of these factors affect those of low socioeconomic status more greatly than those of high socioeconomic status, marking a reduced risk of cancer. Lack of access to both fresh foods and knowledge of BPA exposure as a cancer risk are likely to affect the population as a whole, regardless of socioeconomic status. Affinity characteristics are another factor that may contribute to individuals participating in activities that increase their exposure risk, such as with smoking. Affinity characteristics are shared traits and lifestyle choices seen within populations of like individuals. Those who are new to the population, such as children, will adopt these traits in order to maintain their identity within the group. For example, a child who grows up in a family of tobacco smokers is more likely to smoke themselves. In this way, the exposure activity is perpetuated within the family.

In the case of living in an area where exposure to carcinogens is higher, such as in the Hudson River Valley, factors such as financial restraints, familial ties, and affinity characteristics are also at play. Financial restraints may prevent individuals from leaving an area as they may be unable to afford the move. Individuals may also be bound by proximity to family and those with which they share affinity characteristics. Proximity to family may provide financial and emotional

support while affinity characteristics may provide a sense of identity and belonging. Some notable affinity characteristics include lifestyle, occupation, and linguistic representation.

Future Studies

The results presented in Chapter 2 are preliminary for the investigation of the role of GPER1 in BPA-induced SG formation. Much work is necessary to elucidate this mechanism and determine the role of GPER1 in this pathway.

As mentioned in the previous chapter, this epidemiological study relies on the unstudied assumption that individuals living in poverty consume more canned foods than those living above the poverty line. This marks a large area for further research into the link between canned foods, socioeconomic status, and cancer risk. Additionally, studies to assess the effect of confounding variables such as access to healthcare, degree of urbanization, and workplace exposures on the findings in this study may help illuminate factors not highlighted in this study. Finally, expansion of the model used in this study to investigate FRCs and socioeconomic studies in other US states and potentially other countries could provide additional insight into the scale of this correlation.

References

Appenzeller-Herzog, C. and Hall, M. N. (2012). *Bidirectional crosstalk between endoplasmic reticulum stress and mTOR signaling. Trends Cell Biol.; 22(5): 274-282*. DOI: 10.1016/j.tcb.2012.02.006.

Cancer Mapping Data: 2011-2015. (2018). Health.data.ny.gov. Retrieved December 2, 2022 from https://health.data.ny.gov/Health/Cancer-Mapping-Data-2011-2015/y4pv-ib8r.

Chevalier, N., Bouskine, A., Fenichel, P. (2012). *Bisphenol A promotes testicular seminoma cell proliferation through GPER/GPR30. Int J Cancer*; *130:241–242.* DOI: 10.1002/ijc.25972.

Chen, D., Kannan, K., Tan, H., et al. (2019). *Bisphenol Analogues Other Than BPA: Environmental Occurrence, Human Exposure, and Toxicity, A Review. Environ Sci & Technol.; 50(11): 5438-5453*. https://pubs.acs.org/doi/10.1021/acs.est.5b05387

Cui, A., Li, J., Ron, D., et al. (2011). *The structure of PERK kinase domain suggests the mechanism for its activation. Acta Cryst, D67; 423-428*. doi:10.1107/S0907444911006445

DeLeon, C., Wang, D. Q.-H., and Arnatt, C. K. (2020). *G Protein-Coupled Estrogen Receptor, GPER1, Offers a Novel Target for the Treatment of Digestive Diseases. Front Endocrinol.; 11: 578536.* DOI: 10.3389/fendo.2020.578536

PCBs and Human Health. (n.d.) U.S. Environmental Protection Agency. Retrieved April 7, 2023 from https://www3.epa.gov/hudson/humanhealth.htm#:~:text=PCBs%20are%20probable%20human%20carcinogens,PCBs%20and%20an%20individual's%20exposure.

Fay, M. M., Columbo, D., Cotter, C., wt al. (2021). *Bisphenol A promotes stress granule assembly and modulates the integrated stress response. The Company of Biologists; 10(1).* doi:10.1242/bio.057539

Food Environment Atlas. (2022). USDA Economic Research Service. Retrieved December 2, 2022 from https://www.ers.usda.gov/data-products/food-environment-atlas/go-to-the-atlas/

Friend, C., Hoppe, M, and Wu, J. (2018). *Stressed Out! Effects of Bisphenols on the Cellular Stress Response. Worcester Polytechnic Institute.* E-project-042518-124022

Fuentes, N. and Silveyra, P. (2019). *Estrogen receptor signaling mechanisms. Adv Protein Chem Struct Biol.; 116: 135-170.* doi:10.1016/bs.apcsb.2019.01.001.

Ge, L.-C., Chen, Z.-J., Liu, H., et al. (2014). *Signaling related with biphasic effects of bisphenol A (BPA) on Sertoli cell proliferation: a comparative proteomic analysis. Biochim Biophys Acta - Gen Subj.;* 1840: 2663–2673. DOI: 10.1016/j.bbagen.2014.05.018.

Hanafi, N. I., Kadir, S. H. S. A., Musa, M., et al. (2019). *Low concentration of bisphenol A induces proliferation of gastric cancer cells, HGC-27. J Teknol.; 81: 115–121.* DOI: 10.11113/jt.v81.13670.

Hartle, J. C., Navas-Acien, and Lawrence, R. S. (2016). *The consumption of canned food and*

beverages and urinary Bisphenol A concentrations in NHANES 2003-2008. Environ. Res.; 150: 375-382. DOI: 10.1016/j.envres.2016.06.008

Health Facility Map. (2023). Health.data.ny.gov. Retrieved March 31, 2023 from https://health.data.ny.gov/Health/Health-Facility-Map/875v-tpc8

Ho Vo, D.-K., Hartig, R., Weinert, S., et al. (2019). *G-Protein-Coupled Estrogen Receptor (GPER)-Specific Agonist G1 Induces ER Stress Leading to Cell Death in MCF-7 Cells. Biomolecules; 9(9), 503;* https://doi.org/10.3390/biom9090503

Hui, L., Li, H., Lu, G., et al. (2018). *Low dose of bisphenol A modulates ovarian cancer gene expression profile and promotes epithelial to mesenchymal transition via canonical wnt pathway. Toxicol Sci.; 164: 527–538.* DOI: 10.1093/toxsci/kfy107.

Jeong, J. S., Nam, K. T., Lee, B., et al. (2017). *Low-dose bisphenol A increases bile duct proliferation in juvenile rats: a possible evidence for risk of liver cancer in the exposed population? Biomol Ther.; 25: 545–552.* DOI: 10.4062/biomolther.2017.148.

Khan, N. G., Correia, J., Adiga, D., et al. (2021). *A comprehensive review on the carcinogenic potential of bisphenol A: clues and evidence. Environ Sci Pollut Res Int.; 28(16): 19643–19663.* DOI: 10.1007/s11356-021-13071-w

Lee, P. N., Forey, B. A., and Coombs, K. J., (2012). *Systematic review with meta-analysis of the epidemiological evidence in the 1900s relating smoking to lung cancer. BMC Cancer; 12(385).* DOI: https://doi.org/10.1186/1471-2407-12-385

Ma, X. F., Zhang, J., Shuai, H. L., et al. (2015). *IKKβ/NF-κB mediated the low doses of bisphenol A induced migration of cervical cancer cells. Arch Biochem Biophys.; 573: 52–58.* DOI: 10.1016/j.abb.2015.03.010.

Mesothelioma. (n.d.) Mayo Clinic. Retrieved April 24, 2023 from https://www.mayoclinic.org/diseases-conditions/mesothelioma/symptoms-causes/syc-20375022

Pfeifer, D., Chung, Y. M., Hu, M. C.-T. (2015). *Effects of low-dose bisphenol A on DNA damage and proliferation of breast cells: the role of c-Myc. Environ Health Perspect.;* 123: 1271–1279. doi: 10.1289/ehp.1409199.

Prins, G. S., Hu, W.-Y., Shi, et al. (2014). *Bisphenol A promotes human prostate stem-progenitor cell self-renewal and increases in vivo carcinogenesis in human prostate epithelium. Endocrinology; 155: 805–817.* DOI: 10.1210/en.2013-1955.

Qu, W., Zhao, Z., Chen, S., et al. (2018). *Bisphenol A suppresses proliferation and induces apoptosis in colonic epithelial cells through mitochondrial and MAPK/AKT pathways. Life Sci.; 208: 167–174.* DOI: 10.1016/j.lfs.2018.07.040.

Sauer, S. J., Tarpley, M., Shah, I., et al. (2017). *Bisphenol A activates EGFR and ERK promoting proliferation, tumor spheroid formation and resistance to EGFR pathway inhibition in estrogen receptor-negative inflammatory breast cancer cells. Carcinogenesis.; 38: 252–260.* DOI: 10.1093/carcin/bgx003.

Song, H., Zhang, T., Yang, P., et al. (2015). *Low doses of bisphenol A stimulate the proliferation breast cancer cells via ERK1/2/ERRγ signals. Toxicol Vitr.; 30: 521–528.* DOI: 10.1016/j.tiv.2015.09.009.

Wang, K. H., Kao, A. P., Chang, C. C., et al. (2015). *Bisphenol A-induced epithelial to mesenchymal transition is mediated by cyclooxygenase-2 up-regulation in human endometrial carcinoma cells. Reprod Toxicol.; 58: 229–233.* DOI: 10.1016/j.reprotox.2015.10.011.

Wang, Z., Liu, H., Liu, S. (2017). *Low-dose bisphenol A exposure: a seemingly instigating carcinogenic effect on breast cancer. Adv Sci., 4:1600248.* DOI: 10.1002/advs.201600248.

Wang, K., Zhao, Z., Ji, W. (2019). *Bisphenol A induces apoptosis, oxidative stress and inflammatory response in colon and liver of mice in a mitochondria-dependent manner. Biomed Pharmacother.; 117: 109182.* DOI: 10.1016/j.biopha.2019.109182.